Soft versus hard dynamics for field-driven solid-on-solid interfaces

2002 J. Phys. A: Math. Gen. 35 L117

(http://iopscience.iop.org/0305-4470/35/9/102)

INSTITUTE OF PHYSICS PUBLISHING JOURNAL OF PHYSICS A: MATHEMATICAL AND GENERAL

J. Phys. A: Math. Gen. **35** (2002) L117–L123 PII: S0305-4470(02)31609-3

LETTER TO THE EDITOR

Soft versus hard dynamics for field-driven solid-on-solid interfaces

P A Rikvold[1,2] **and M Kolesik**[3,4]

[1] Center for Materials Research and Technology, School of Computational Science and Information Technology, and Department of Physics, Florida State University, Tallahassee, FL 32306-4351, USA
[2] Department of Fundamental Sciences, Faculty of Integrated Human Studies, Kyoto University, Kyoto 606, Japan
[3] Institute of Physics, Slovak Academy of Sciences, Bratislava, Slovak Republic
[4] Department of Mathematics, University of Arizona, Tucson, AZ 85721, USA

E-mail: rikvold@csit.fsu.edu, kolesik@acms.arizona.edu

Received 4 December 2001, in final form 2 January 2002
Published 22 February 2002
Online at stacks.iop.org/JPhysA/35/L117

Abstract

Analytical arguments and dynamic Monte Carlo simulations show that the microscopic structure of field-driven solid-on-solid interfaces depends strongly on the details of the dynamics. For non-conservative dynamics with transition rates that factorize into parts dependent only on the changes in interaction energy and field energy, respectively (soft dynamics), the intrinsic interface width is field independent. For non-factorizing rates, such as the standard Glauber and Metropolis algorithms (hard dynamics), it increases with the field. Consequences for the interface velocity and its anisotropy are discussed.

PACS numbers: 68.35.Ct, 05.10.Ln, 68.43.Jk, 75.60.Jk

Surfaces and interfaces moving under far-from-equilibrium conditions are important in the formation of patterns and structures. For example, domain growth by the motion of defects such as grain boundaries or dislocations influences the mechanical properties of metals [1] and the structures formed during phase transformations in adsorbate systems [2], while the propagation of domain walls influences the switching dynamics of magnetic nanoparticles and ultrathin films [3]. Recently, interface dynamics was even used to analyse the scalability of discrete-event simulations on parallel computers [4]. The importance of moving interfaces in a wide variety of fields has inspired enormous interest in their structure and dynamics [5]. However, despite the fact that many interface properties, such as mobility and chemical activity, are determined by the *microscopic* structure, interest has mostly focused on the large-scale interface structure and its universal properties. In this letter we show that the microstructure of a moving interface can be dramatically influenced by seemingly minor modifications of

the growth mechanism, with measurable consequences for such macroscopic quantities as the interface velocity and its anisotropy.

The detailed microscopic mechanism of the interface motion is usually not known, and it is therefore common to mimic the essential features in a dynamic Monte Carlo (MC) simulation of a model stochastic process [1]. In doing so, there are two important distinctions that must be made. One is between those transition probabilities that only depend on the energy difference between the initial and final states (often referred to as Metropolis, Glauber or heat-bath rates [6–8]), and those that involve an activation barrier between the two states (often referred to as Arrhenius rates) [2,6,8,9]. Another distinction is between dynamics that do not conserve the order parameter, such as the Metropolis and Glauber single-spin flip algorithms, and conservative dynamics, such as the Kawasaki spin-exchange dynamic [7]. Once it is decided to which of these categories the system belongs, the dynamic is often chosen on the basis of convenience.

It is well known that different microscopic dynamics can yield different equilibration paths and equilibrium fluctuations [10] (cluster versus local MC algorithms being the most extreme example [7]) and even noticeable differences in the steady-state microstructure [6,8]. Nevertheless, the general expectation is that, if no additional parameters (such as an activation barrier or a diffusion rate) are introduced into the physical model, observables are only affected *quantitatively*. However, here we demonstrate striking *qualitative* differences between the microstructural consequences of two different stochastic dynamics that do not involve a transition barrier, even though both obey detailed balance and neither involves order-parameter conserving moves. For this demonstration we use an unrestricted solid-on-solid (SOS) interface [11] separating uniform spin-up and spin-down phases in a ferromagnetic $S = 1/2$ Ising system on a square lattice of unit lattice constant. The interface consists of integer-valued steps parallel to the y-direction, $\delta(x) \in \{-\infty, +\infty\}$, where the step position x is also an integer. Its energy is given by the nearest-neighbour Ising Hamiltonian with anisotropic ferromagnetic interactions, J_x and J_y in the x- and y-directions, respectively: $\mathcal{H} = -\sum_{x,y} s_{x,y}\left(J_x s_{x+1,y} + J_y s_{x,y+1} + H\right)$. The two states at site (x, y) are denoted by the spin $s_{x,y} = \pm 1$, $\sum_{x,y}$ runs over all sites, and H is the applied field. We take $s_{x,y} = -1$ on the side of the interface corresponding to large positive y, so that the interface on average moves in the positive y-direction for $H > 0$. In the equivalent lattice-gas language, $s_{x,y} = +1$ corresponds to solid and $s_{x,y} = -1$ to gas or liquid, and H is proportional to a chemical-potential imbalance. The interface evolves through single spin flips (in lattice-gas language: adsorption/desorption events) that occur with probability $W[\beta\Delta E]$ where ΔE is the energy change that would result from the transition, constrained by the requirement that the probabilities obey detailed balance (see [12, 13] for details). To restrict the accessible configurations to a simple SOS interface without bubbles or overhangs, transitions are allowed only for spins that have one single broken bond in the y-direction. Regardless of the details of the transition probabilities, which lead to dramatic *microscopic* structural differences as demonstrated below, the *macroscopic* structure of the interfaces belongs to the Kardar–Parisi–Zhang (KPZ) dynamic universality class [5,14]. We emphasize that the absence of energy barriers and order-parameter conserving diffusion (spin-exchange) moves sets our model clearly apart from commonly studied models of molecular beam epitaxy (MBE) [6,8]. It is closely similar to the diffusion-free dynamical model studied in three dimensions in [15] which, however, does not consider the microscopic interface structure in detail.

Recently [12] we introduced a mean-field approximation for the driven-interface microstructure, in which the probability density function (pdf) for the height of a single step takes the Burton–Cabrera–Frank (BCF) form [11]

$$p[\delta(x)] = Z^{-1} X^{|\delta(x)|}\, \mathrm{e}^{\gamma(\phi)\delta(x)} \tag{1}$$

where the Lagrange multiplier $\gamma(\phi)$ enforces $\langle\delta(x)\rangle = \tan\phi$ independent of x, corresponding to an overall angle ϕ between the interface and the x-axis. The width parameter X, which for a driven interface can depend on both H and the temperature T, is discussed below. The partition function in (1) is

$$Z(\phi) = \sum_{\delta=-\infty}^{+\infty} X^{|\delta|} \mathrm{e}^{\gamma(\phi)\delta} = \frac{1 - X^2}{1 - 2X\cosh\gamma(\phi) + X^2} \tag{2}$$

with

$$\mathrm{e}^{\gamma(\phi)} = \frac{\left(1 + X^2\right)\tan\phi + \sqrt{\left(1 - X^2\right)^2 \tan^2\phi + 4X^2}}{2X\,(1 + \tan\phi)}\,. \tag{3}$$

For $\phi = 0$, $\gamma(\phi) = 0$, yielding $Z(0) = (1 + X)/(1 - X)$.

In the approximation of [12], individual steps are assumed to be statistically independent (as in the original BCF model for *equilibrium* interfaces). The width parameter X is then obtained self-consistently as [12, 13]

$$X(T, H) = X_0(T) \left\{ \frac{\mathrm{e}^{-2\beta H} W[\beta(-2H - 4J_x)] + \mathrm{e}^{2\beta H} W[\beta(+2H - 4J_x)]}{W[\beta(-2H - 4J_x)] + W[\beta(+2H - 4J_x)]} \right\}^{1/2} \tag{4}$$

where $X_0(T) \equiv \mathrm{e}^{-2\beta J_x}$, with $\beta = 1/k_\mathrm{B}T$ (k_B is Boltzmann's constant), is the BCF zero-field equilibrium value of X. For $H = 0$, $X(T, H)$ reduces to $X_0(T)$. For instance, using the Glauber transition probability

$$W_\mathrm{G}(s_{x,y} \to -s_{x,y}) = \frac{\mathrm{e}^{-\beta\Delta E}}{1 + \mathrm{e}^{-\beta\Delta E}} \tag{5}$$

we get

$$X_\mathrm{G}(T, H) = X_0(T) \left\{ \frac{\mathrm{e}^{2\beta J_x}\cosh(2\beta H) + \mathrm{e}^{-2\beta J_x}}{\mathrm{e}^{-2\beta J_x}\cosh(2\beta H) + \mathrm{e}^{2\beta J_x}} \right\}^{1/2}. \tag{6}$$

Equation (5) exemplifies a class of dynamics known as *hard* in the literature on nonequilibrium lattice models [16], in which the transition probabilities depend directly on the total energy change, ΔE. In a different class, known as *soft*, the probabilities factorize into a part due only to the change in the field energy, $\Delta E_H \propto H$, and a part due only to the change in the interaction energy, $\Delta E_J \propto J_x$. One example is the *soft Glauber dynamic*

$$W_\mathrm{SG}(s_{x,y} \to -s_{x,y}) = \frac{\mathrm{e}^{-\beta\Delta E_H}}{1 + \mathrm{e}^{-\beta\Delta E_H}} \frac{\mathrm{e}^{-\beta\Delta E_J}}{1 + \mathrm{e}^{-\beta\Delta E_J}} \tag{7}$$

which also obeys detailed balance.

The important point is that when a factorizing transition probability such as (7) is used in (4), all dependence on H cancels due to the detailed balance. Whether one uses a soft or a hard dynamic thus strongly affects the intrinsic interface width and properties that depend on it, such as the propagation velocity. The need to use a soft dynamic in cases where the 'field' represents a chemical-potential difference has been recognized in some MC studies of crystal growth [17–19].

Next we illustrate the large differences between hard and soft dynamics by comparing analytic approximations and dynamic MC simulations of driven SOS interfaces with J_x=J_y=J, using the hard and soft Glauber dynamics, respectively. In particular, we consider the field and temperature dependences of the intrinsic interface width, represented by the average absolute value of the step height, and the resulting interface velocity and its anisotropy.

In figure 1 we show numerical evidence supporting our predictions for the average step height, which for $\phi = 0$ is related to X as $\langle|\delta|\rangle = 2X/(1 - X^2)$, under both the hard and

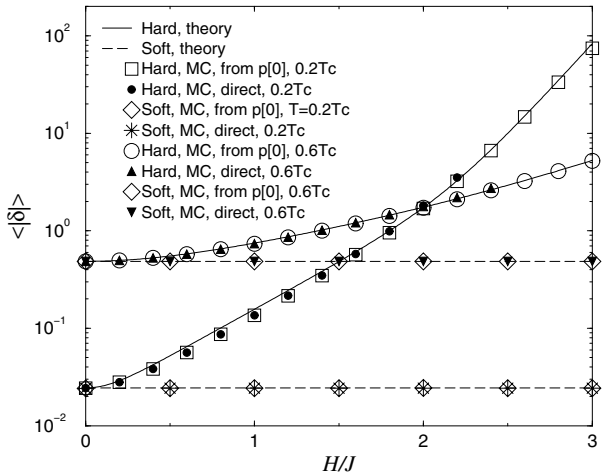

Figure 1. Average step height $\langle|\delta|\rangle$ versus H for ϕ=0 at T=0.2T_c and 0.6T_c, where T_c is the exact Ising critical temperature. Solid curves, obtained as $\langle|\delta|\rangle = 2X/(1-X^2)$ with $X = X_G(T, H)$, are theoretical predictions for the hard dynamic. Dashed lines, similarly obtained with $X = X_0(T)$, are theoretical predictions for the soft dynamic. The MC data are from direct summation over the simulated single-step pdfs (filled symbols) and from $p[0]$ using $\langle|\delta|\rangle = \left\{p[0]^{-1} - p[0]\right\}/2$ (empty symbols). In this and the following figures, the statistical uncertainty is much smaller than the symbol size.

Table 1. The three spin classes that contribute to the interface velocity in the SOS model (column 1), together with the corresponding energy changes resulting from a successful spin flip (column 2, with upper sign corresponding to initial $s = -1$ and lower sign to $s = +1$), the average class populations for general tilt angle ϕ (column 3) and for $\phi = 0$ (column 4), and the contributions to the interface velocity in the y-direction for the hard Glauber dynamic (column 5) and for the soft Glauber dynamic (column 6). In columns 3 and 4, X corresponds to the width parameter $X(T, H)$ for the specific dynamic used, given by (4) in the general case, (6) for the hard Glauber dynamic, and $X_0(T) = e^{-2\beta J_x}$ for soft dynamics.

Class	ΔE	$\langle n(js)\rangle$, general ϕ	$\langle n(js)\rangle$, $\phi = 0$	$\langle v_y(js)\rangle_G$	$\langle v_y(js)\rangle_{SG}$
$0s$	$\mp 2H + 4J_x$	$\frac{1-2X\cosh\gamma(\phi)+X^2}{(1-X^2)^2}$	$\frac{1}{(1+X)^2}$	$\frac{\tanh(\beta H)}{1+\left[\frac{\sinh(2\beta J_x)}{\cosh(\beta H)}\right]^2}$	$\frac{\tanh(\beta H)X_0^2}{1+X_0^2}$
$1s$	$\mp 2H$	$\frac{2X[(1+X^2)\cosh\gamma(\phi)-2X]}{(1-X^2)^2}$	$\frac{2X}{(1+X)^2}$	$\tanh(\beta H)$	$\frac{1}{2}\tanh(\beta H)$
$2s$	$\mp 2H - 4J_x$	$\frac{X^2[1-2X\cosh\gamma(\phi)+X^2]}{(1-X^2)^2}$	$\frac{X^2}{(1+X)^2}$	$\frac{\tanh(\beta H)}{1+\left[\frac{\sinh(2\beta J_x)}{\cosh(\beta H)}\right]^2}$	$\frac{\tanh(\beta H)}{1+X_0^2}$

soft Glauber dynamics at two different temperatures. (Simulational details are given below.) The difference between the two dynamics is striking: the step heights for the soft dynamic are independent of H, in contrast to the strong H dependence produced by the hard dynamic. Additional confirmation of the functional form of the single-step pdf (1) is obtained from the MC data by calculating $\langle|\delta|\rangle$, both directly by summation over the numerically obtained pdf and from the probability of zero step height for $\phi = 0$ as $\langle|\delta|\rangle = \left\{p[0]^{-1} - p[0]\right\}/2$. This result is obtained by combining $p[0] = Z^{-1}$ with the above relation for $\langle|\delta|\rangle$ in terms of X.

The spins in an Ising system can be classified by the value of ΔE, which is uniquely determined by s and the number of broken x- and y-bonds. The active spin classes all have one broken y-bond and can be labelled by s=$\pm$1 and the number of broken x-bonds, $j \in \{0, 1, 2\}$, as js. The classes and corresponding ΔE are given in the first two columns of table 1. The

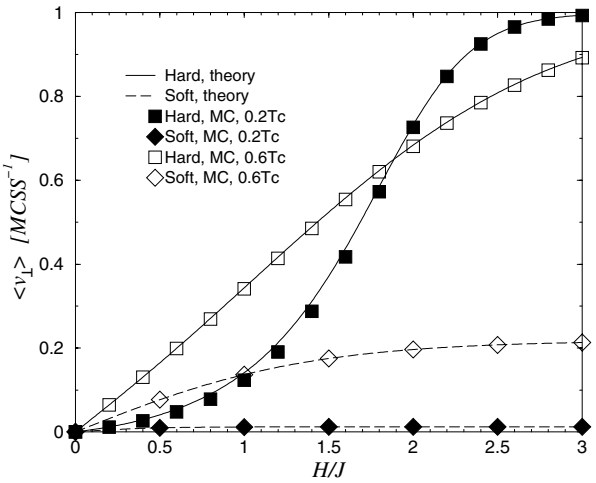

Figure 2. The perpendicular interface velocity $\langle v_\perp \rangle$ versus H for $\phi = 0$ at T=0.2T_c and 0.6T_c. Theoretical results for the hard dynamic are from (9) (solid curves) with MC data shown as squares. Theoretical results for the soft dynamic are from (10) (dashed curves) with MC data shown as diamonds.

details of our 'active-site' implementation of the spin-class-based discrete-time n-fold way algorithm [20] are given in [12], the only difference here being the restriction to flips only at sites with one broken y-bond. The data shown here are for interfaces of size $L_x = 10^4$ in the x-direction, which were allowed 5000 n-fold way updates per active site to reach stationarity, after which pdfs, class populations and velocities were collected over 50 000 updates per active site.

Assuming up–down symmetry of the interface, the mean perpendicular propagation velocity is given by

$$\langle v_\perp(T, H, \phi)\rangle = \cos\phi \sum_j \langle n(js)\rangle \langle v_y(j)\rangle \tag{8}$$

in units of inverse MC steps per site (MCSS^{-1}). Here, the average spin-class populations, $\langle n(js)\rangle$, are calculated from the single-step pdf, assuming statistical independence [12], and the results are given in the third and fourth columns of table 1. The corresponding contributions to the interface velocity in the y-direction, $\langle v_y(j)\rangle = \{W[\beta\Delta E(j-)] - W[\beta\Delta E(j+)]\}$, are given in the fifth and sixth columns of table 1 for the hard and soft Glauber dynamic, respectively. The special case of $\phi = 0$ leads to compact formulae:

$$\langle v_\perp(T, H, 0)\rangle_{\mathrm{G}} = \frac{\tanh(\beta H)}{(1+X)^2}\left\{2X + \frac{1+X^2}{1+\left[\frac{\sinh(2\beta J_x)}{\cosh(\beta H)}\right]^2}\right\} \tag{9}$$

with X from (6) for the hard Glauber dynamic, and

$$\langle v_\perp(T, H, 0)\rangle_{\mathrm{SG}} = \tanh(\beta H)\frac{X_0}{1+X_0^2} \tag{10}$$

for the soft Glauber dynamic. These results are compared with the corresponding MC data in figure 2. The difference between the two dynamics is clear.

The angular dependencies of $\langle v_\perp\rangle$ for the two dynamics are illustrated in figure 3. The theoretical results represent (8) with terms from table 1. The hard dynamic yields an anisotropy

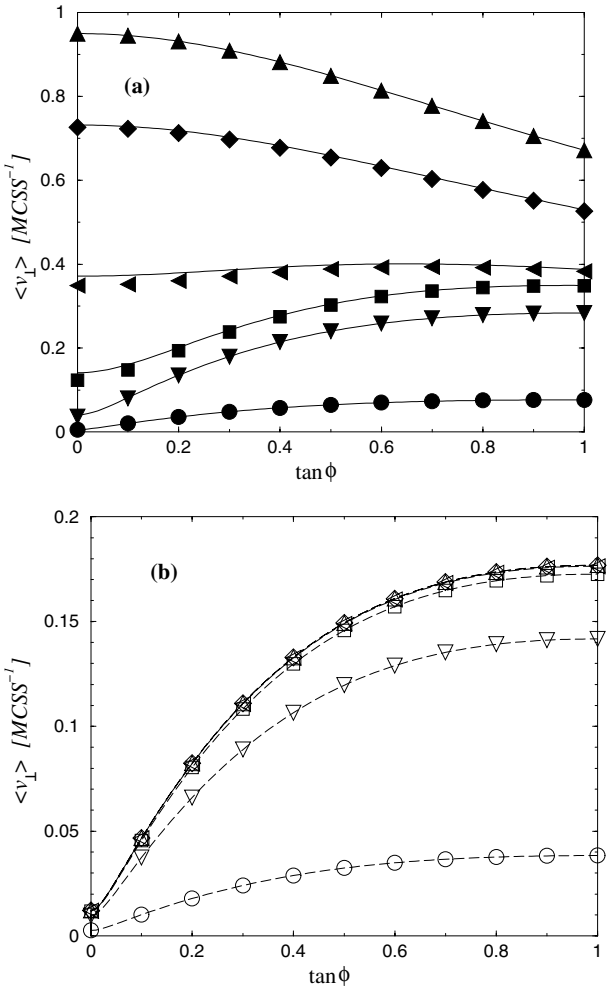

Figure 3. Angle dependence of the perpendicular interface velocity $\langle v_\perp \rangle$ at T=0.2T_c for (a) hard dynamic, (b) soft dynamic, for (from bottom to top) $H/J = 0.1, 0.5, 1.0, 1.5, 2.0$, and 2.5. Curves are theoretical predictions, data points MC results. On this scale, the soft-dynamic results overlap for $H/J \geqslant 1.5$.

which changes from that of the single-step model [5] for weak H, to the reverse anisotropy of the Eden model [21, 22] for strong H. There is no such change for the soft dynamic, which shows a single-step-like anisotropy for all fields. Effects of different transition probabilities on nonequilibrium growth shapes have already been observed in systems with conserved order parameter [10]. It is likely that the different anisotropies resulting from the hard and soft dynamics will lead to different growth shapes in the case of nonconserved order parameter as well.

With hard dynamics, the up–down symmetry of the interface is gradually destroyed with increasing field [4, 12, 13, 23], leading to different class populations for $s = +1$ and $s = -1$. Our MC simulations show this skewness to be absent for the soft dynamic. This makes us believe that the field dependence in (10) is exact in the following sense. If the interface has up–down symmetry and is driven with a soft dynamic, then the generated interface shapes are independent of H. Consequently, the only dependence of the velocity on H is in the difference

between the spin-flip probabilities of a down spin and an up spin, which yields $\tanh(\beta H)$ for the Glauber dynamic.

In summary, we have presented analytical and dynamic MC results that show remarkable qualitative differences in the microscopic structure of field-driven SOS interfaces in the KPZ dynamic universality class, depending on whether the local stochastic spin dynamic is hard (such as the standard Glauber and Metropolis dynamics) or soft. In the former case, $\langle|\delta|\rangle$ depends strongly on H, while in the latter it has no H dependence at all. We emphasize that the difference between the hard and soft dynamic is purely dynamical and does *not* involve introduction into the physical model of any new parameters, such as an activation barrier or a diffusion rate. If microstructural information is desired from a dynamic MC simulation, great care must therefore be exercised, both in choosing the transition probabilities and in interpreting the results. Analogous effects for other models, such as Ising interfaces [12], and in three dimensions, and the possibility that the resulting growth shapes may be different [10], are left for future study. Further details on the microstructure of the SOS interface under the hard Glauber dynamic will be reported elsewhere [13].

We thank G Brown, G Buendía, S J Mitchell, M A Novotny, and K Park for useful comments. PAR appreciates hospitality at Kyoto University. Supported in part by US NSF Grant No DMR-9981815, and by Florida State University through MARTECH and CSIT.

References

[1] Mendelev M I and Srolovitz D J 2000 *Acta Mater.* **48** 3711
Mendelev M I and Srolovitz D J 2001 *Acta Mater.* **49** 589
Mendelev M I and Srolovitz D J 2001 *Acta Mater.* **49** 2843
[2] Mitchell S J, Brown G and Rikvold P A 2001 *Surf. Sci.* **471** 125
[3] Rikvold P A, Brown G, Mitchell S J and Novotny M A *Nanostructured Magnetic Materials and their Applications* ed D Shi, B Aktas, L Pust and F Mikailov (Berlin: Springer) at press (cond-mat/0110103)
[4] Korniss G, Toroczkai Z, Novotny M A and Rikvold P A 2000 *Phys. Rev. Lett.* **84** 1351
[5] Barabási A-L and Stanley H E 1995 *Fractal Concepts in Surface Growth* (Cambridge: Cambridge University Press) and references therein
[6] Siegert M and Plischke M 1994 *Phys. Rev.* E **50** 917
[7] Landau D P and Binder K 2000 *Monte Carlo Simulations in Statistical Physics* (Cambridge: Cambridge University Press)
[8] Shim Y and Landau D P 2001 *Phys. Rev.* E **64** 036110
[9] Kang H C and Weinberg W H 1989 *J. Chem. Phys.* **90** 2824
Fichthorn K A and Weinberg W H 1991 *J. Chem. Phys.* **95** 1090
[10] Shochet O, Kassner K, Ben-Jacob E, Lipson S B and Müller-Krumbhaar H 1992 *Physica* A **181** 136 and references therein
[11] Burton W K, Cabrera N and Frank F C 1951 *Phil. Trans. R. Soc. (Lond.)* A **243** 299
[12] Rikvold P A and Kolesik M 2000 *J. Stat. Phys.* **100** 377
[13] Rikvold P A and Kolesik M 2002 in preparation
[14] Kardar M, Parisi G and Zhang Y-Z 1986 *Phys. Rev. Lett.* **56** 889
[15] Jiang Z and Ebner C 1992 *Phys. Rev.* B **45** 6163
[16] Marro J and Dickman R 1999 *Nonequilibrium Phase Transitions in Lattice Models* (Cambridge: Cambridge University Press) ch 7
[17] Guo H, Grossmann B and Grant M 1990 *Phys. Rev. Lett.* **64** 1262
[18] Kotrla M and Levi A C 1991 *J. Stat. Phys.* **64** 579
[19] Hontinfinde F, Krug J and Touzani M 1997 *Physica* A **237** 363
[20] Bortz A B, Kalos M H and Lebowitz J L 1975 *J. Comput. Phys.* **17** 10
[21] Meakin P, Jullien R and Botet R 1986 *Europhys. Lett.* **1** 609
[22] Hirsch R and Wolf D E 1986 *J. Phys. A: Math. Gen.* **19** L251
[23] Neergaard J and den Nijs M 1997 *J. Phys. A: Math. Gen.* **30** 1935